

# Quantifying the Knudsen force on heated microbeams: A compact model and direct comparison with measurements

Jeremy Nabeth, Sruti Chigullapalli, and Alina A. Alexeenko

*School of Aeronautics and Astronautics, Purdue University, West Lafayette, Indiana 47907, USA*

(Received 5 March 2010; revised manuscript received 14 March 2011; published 10 June 2011)

At the microscale, even moderate temperature differences leading to thermal nonequilibrium can result in significant Knudsen forces generated by the energy exchange between gas molecules and solids immersed in a gas. Experimental measurements of the microscale Knudsen force have been reported by Passian *et al.*, *Phys. Rev. Lett.* **90**, 124503 (2003) using heated microcantilevers of atomic force microscope probes. The present study investigates the mechanism and magnitude of Knudsen forces in detail based on numerical solution of the Boltzmann kinetic equation with the ellipsoidal statistical Bhatnagar-Gross-Krook approximation for the collisional relaxation process. A direct comparison between the numerical simulations and experimental measurements is presented. We show that, assuming a fully diffuse interaction of gas molecules with the surfaces of the heated cantilever, simulations agree with measurements for different operating pressures in argon and nitrogen ambients. For the helium ambient the simulations agree with measurements only when an incomplete accommodation is used. A closed-form model for the nondimensional Knudsen force coefficient on a heated microbeam is obtained that can be used for quantifying such forces in analysis and design of microsystems under a wide range of geometrical, thermal, and pressure conditions.

DOI: [10.1103/PhysRevE.83.066306](https://doi.org/10.1103/PhysRevE.83.066306)

PACS number(s): 47.61.-k, 47.45.Gx, 51.20.+d, 51.90.+r

## I. INTRODUCTION

Knudsen forces arise in systems when there is a thermal gradient with a characteristic length scale comparable to the molecular mean free path in the ambient gas. Forces on unequally heated vanes, such as in Crookes radiometer [1], are referred to as radiometric [2] or thermomolecular [3] and have been observed and studied in vacuum systems [4]. Although large temperature differences are difficult to sustain across micron-sized objects, a similar force can be created on, say, a heated microbeam immersed in a colder gas. Recently, measurements of the Knudsen force at the microscale have been obtained using heated atomic force microscopy probes [5,6]. Exploiting such forces on microstructures in the presence of thermal gradients can provide a unique actuation mechanism for mass detection, thermogravimetry, and very high resolution heat flux measurements.

Measuring Knudsen forces precisely at the microscale is an arduous task. Since only limited analytical results exist, numerical simulations can provide a basis for understanding the physical mechanisms governing the generation of Knudsen forces. Recently, numerical simulations of rarefied gas flows around heated microbeams were obtained using the deterministic finite-difference–discrete-velocity method [7] and the direct simulation Monte Carlo method [8]. Qualitative trends similar to those observed in experiments by Passian *et al.* were obtained; however, quantitative comparison was not available. Here we compare directly the numerical simulations with the experimental measurements for heated microbeams and obtain a closed-form model for the Knudsen force applicable for a wide range of conditions beyond the existing theories [9,10] for strictly free molecular flow. Zhu *et al.* [8] observed negative Knudsen forces near  $\text{Kn} = 1$  and from  $\text{Kn} = 1.5$  to  $\text{Kn} = 30$  and found that thermal edge flow is the main driving force. Note that they used a gap size that was half of the beam thickness and also used a temperature difference an order

of magnitude greater than the experiments by Passian. No such negative trend was observed in the experiments or in our simulations.

Qualitatively, the phenomenon of Knudsen force can be understood by considering a hot beam in the vicinity of a cold substrate. As shown in Fig. 1, the beam is closer to the substrate than to the upper boundary of the domain. Hence, the gradient of gas temperature below the beam is greater than the one above. Now consider two molecules located one mean free path away from the beam. The molecule above the beam will bounce and give an impulse in the negative  $y$  direction, whereas the one below the beam will give an impulse in the upward direction. Note that any gain in momentum would be upon the actual collision with the surface. According to the difference in gradients of temperature, the incident molecule below the beam will be in a colder area since the temperature drops substantially faster. Therefore, the molecule colliding with the bottom surface of the beam will experience a smaller gain in momentum than the one coming from above the beam. Consequently, the resulting momentum given to the beam will be in the direction of negative  $y$  axis, but in reality the beam tends to move upward. This is because of the difference in the number of molecules per unit time that hit the bottom and top of the surface, as is seen in the vortices in Fig. 2(a). There is no space available for bottom vortices to be created; therefore, the top vortices result in fewer molecules hitting the surface (with downward components to their momenta), and the bottom molecules push the beam up because of their greater flux onto the surface.

## II. SIMULATION APPROACH

Quantitatively, the Knudsen force can be calculated by using a numerical solution of the Boltzmann kinetic equation for the velocity distribution function of gas molecules. Here we

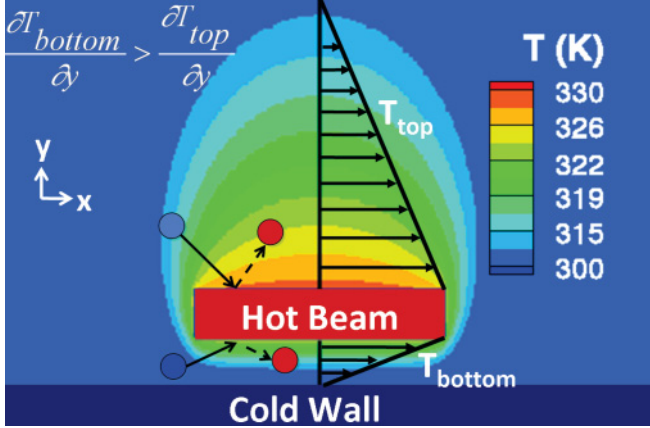


FIG. 1. (Color online) Two-dimensional schematic of the Knudsen force generation on a heated beam near a substrate. The gradient of temperature in the  $y$  direction is higher on the bottom of the beam than on the top. Also shown are two molecules at a distance of one mean free path away from the top and bottom of the beam, which, on collision with the beam, impart a downward force on the beam. Please note that in reality the beam moves upward because of the difference in the number of molecules hitting the top and bottom surfaces.

solve the 2D quasisteady kinetic equation with the ellipsoidal-statistical Bhatnagar-Gross-Krook (ESBGK) collision model:

$$u \frac{\partial f}{\partial x} + v \frac{\partial f}{\partial y} = \frac{f_0 - f}{\tau}, \quad (1)$$

where  $f = f(x, y, u, v, w)$  is the velocity distribution function of gas molecules,  $(x, y)$  are Cartesian coordinates in physical space, and  $(u, v, w)$  are Cartesian-type coordinates in velocity space. The anisotropic Gaussian function  $f_0$  and the collision relaxation parameter  $\tau$  are dependent on the local density, average flow velocity, and stresses in the gas as well as the gas molecular properties, such as the viscosity coefficient [11]. Details of the formulation and numerical implementation can be found in Ref. [12]. While the experimental setup in Ref. [5] corresponds to a three-dimensional flow around a perforated microbeam with two sets of 8- and 2- $\mu\text{m}$  diameter holes, the simulations have been done for a two-dimensional geometry (as shown in Fig. 1) with an equivalent front-to-side area ratio of 10.

The Boltzmann-ESBGK solver employs the finite-volume method (FVM) with a second-order quadrant-splitting scheme applied in the physical space on uniform and nonuniform structured meshes. The velocity space in polar coordinates consists of sixteenth-order Gauss Hermite quadrature in the velocity magnitude and 64 uniform velocity angles. By using the symmetry, only the right half of the domain in Fig. 1 is used for simulations. The left, top, right, and bottom boundaries are symmetry, pressure inlet, pressure inlet, and wall boundaries, respectively. We use a Maxwell model of gas-surface interaction for the wall boundary conditions. The model assumes that, with a probability of  $\alpha$ , a molecule colliding with the wall undergoes a diffuse reflection accommodating to the wall temperature, whereas the rest of collisions, with the probability of  $(1 - \alpha)$ , are specular, with no momentum or energy exchange. The value of  $\alpha$  is also referred to as the accommodation coefficient. We assume a constant  $\alpha$  for the top and bottom

surfaces of the microcantilever. Note that an analytical solution for a heated plate near the wall in the special case of strictly free molecular flow gives a nonzero total force only if the wall accommodation coefficient is less than 1 [9].

Rigorous grid convergence tests were performed for physical and velocity space. A domain convergence study showed that the height and width of the domain have to be larger than 1.5 times the width of the beam. The Richardson extrapolation [13] was used to estimate the accuracy of the solution and has shown that the numerical error is less than 7.5% for all cases considered.

### III. RESULTS AND DISCUSSION

The computed flow fields are shown in Fig. 2(a) for the case of argon gas at a Knudsen number of  $\text{Kn} = 0.45$  and  $\text{Kn} = 5$  at  $\Delta T = 30$  K. The Knudsen number is defined here as the ratio of the mean free path  $\lambda$  in ambient gas to the gap  $g$  between the beam and the substrate,  $\text{Kn} = \lambda/g$ . One can see the creation of a vortex at the corner of the beam that is similar to the one occurring in the thermal edge flow for an unequally heated beam [14]. Figure 3 shows the gradients of temperature below and above the beam. As expected with the qualitative approach, the gradient of temperature is larger below the beam. The Knudsen force is obtained from the simulations by integrating the computed normal stress  $P_{yy}$  along the width of the cantilever cross section and the shear stress  $P_{xy}$  along the thickness of the beam, as shown in Eq. (2).

$$\begin{aligned} P_{yy} &= m \iint \int (v')^2 f du dv dw, \\ P_{xy} &= m \iint \int u'v' f du dv dw. \end{aligned} \quad (2)$$

Here,  $u', v'$  are the molecular thermal velocities,  $u' = u - \bar{u}$ ,  $v' = v - \bar{v}$ , where  $\bar{u}$  and  $\bar{v}$  refer to the mean flow velocities in the  $x$  and  $y$  directions, respectively. The pressure profiles on Figs. 2(b) and 2(c) show that the pressure on the bottom of the beam is larger than the one on the top. Thus, the resulting force on the beam is upward, which agrees with the qualitative approach.

The simulations have been compared with experimental results from Passian *et al.* [5] for a temperature difference  $\Delta T = 30$  K and  $T_0 = 300$  K, as reported in the experimental work, and a constant accommodation coefficient  $\alpha$ , assumed to be the same for the beam and the substrate. When the value of 1.0 is used for  $\alpha$ , the simulations agree with the experimental results for argon and nitrogen ambients [Figs. 4(a) and 4(b)], with a maximum deviation of 3.7% and 9.0%, respectively, both at about  $\text{Kn} = 0.4$ . However, a maximum difference of 82% can be observed for helium at  $\text{Kn} = 0.5$  if complete momentum accommodation is assumed in the simulations. This deviation is attributed to the significantly lower momentum accommodation coefficient  $\alpha$  for the helium gas as compared to nitrogen and argon. The value of  $\alpha$  of about 0.5 has been measured for helium [15] interacting with an aluminum surface. Additional simulations with a reduced accommodation coefficient for helium gas resulted in a much better agreement with the experiments, within about 15%, as shown in Fig. 4(c) for  $\alpha = 0.8$ .

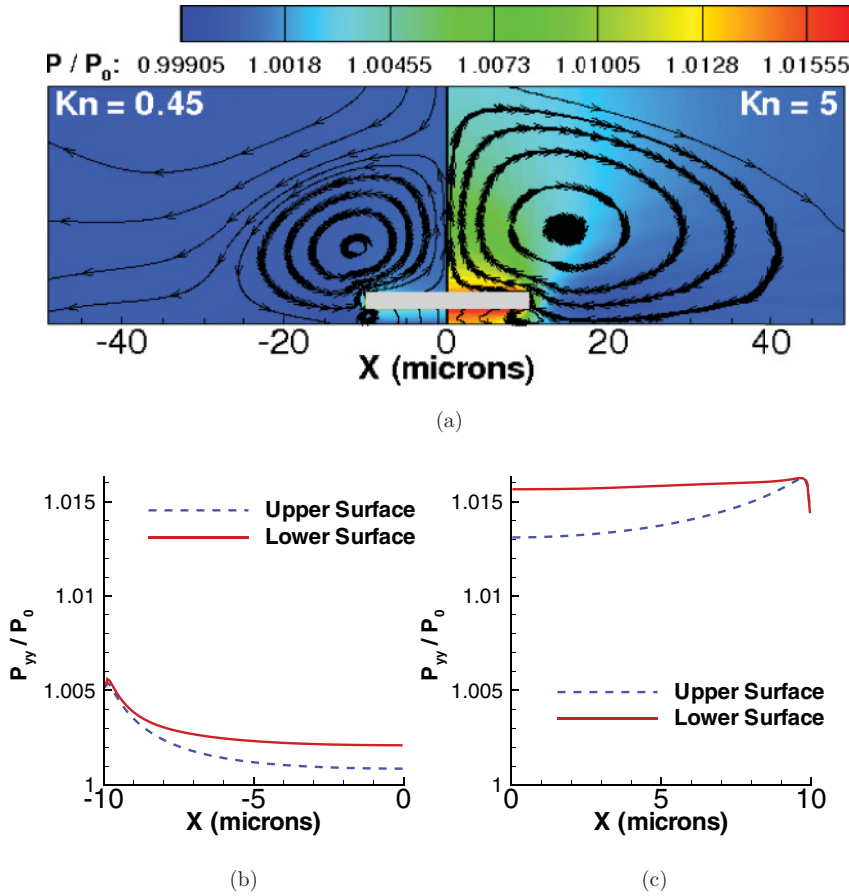


FIG. 2. (Color online) Computed nondimensional pressure distributions. (a) Pressure flow fields and streamlines at (left)  $Kn = 0.45$  and (right)  $Kn = 5$ . The vortex at the corner of the beam results in lowering the normal flux on the top surface and increasing the upward force on the beam. (b) Pressure profile along the beam at  $Kn = 0.45$ . (c) Pressure profile along the beam at  $Kn = 5$ . The pressure on the bottom surface is greater than that on the top surface, thereby resulting in an upward force.

Based on the simulations, a closed-form expression for Knudsen force on a heated beam at a distance  $g$  from a substrate at temperature  $T_0$  for a gas with density  $\rho$ , ratio of specific heats  $\gamma$ , and gas constant  $R$  is developed. Note

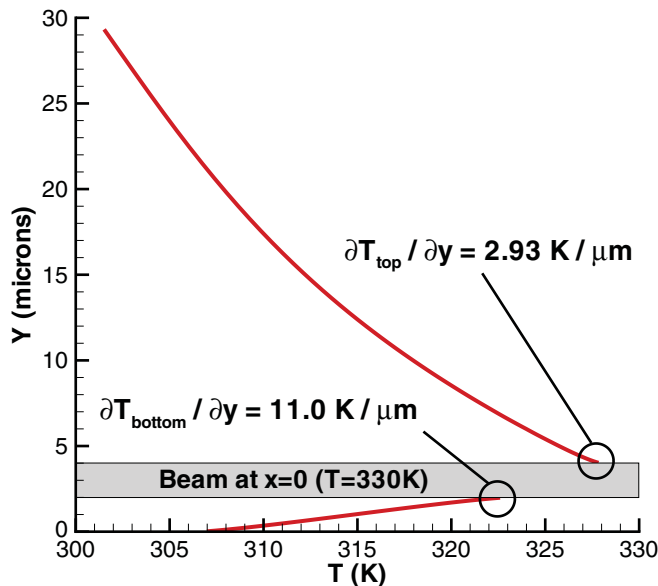


FIG. 3. (Color online) Temperature profiles above and below the beam along the symmetry line  $x = 0$  at  $Kn = 0.48$ . The temperature jump and gradient in the  $y$  direction are higher on the bottom surface than on the top surface.

that, in general, the force coefficient would also depend on the value of the momentum accommodation coefficient, which has been assumed to be constant and equal to 1 here. The dynamic similarity analysis [16] results in the following nondimensional relation:

$$C_{Kn} = \frac{F'_{Kn}}{\rho R \Delta T b} = f\left(\frac{T_0}{\Delta T}, Kn, \frac{t}{g}, \frac{b}{g}, \gamma, \alpha\right), \quad (3)$$

where  $C_{Kn}$  is the Knudsen force coefficient,  $F'_{Kn}$  is the force per unit length on the beam,  $\Delta T$  is the temperature difference between the beam and the substrate,  $Kn$  is the Knudsen number,  $t$  and  $b$  are the thickness and width of the beam, respectively,  $\gamma$  is the heat capacity ratio, and  $\alpha$  is the accommodation coefficient for the gas. Such a nondimensional expression allows us to determine the governing nondimensional parameters for the Knudsen force and is general enough to be applicable in a wide variety of geometrical, thermal, and pressure conditions.

Simulations have been performed for argon, nitrogen, and helium with constant  $\frac{T_0}{\Delta T} = 10$ ,  $\frac{t}{g} = 1$ ,  $\frac{b}{g} = 10$  in order to keep the same constants as in the experiments. The value of  $\alpha$  has been set to 1. Figure 5(a) shows a comparison between simulations and experimental results in terms of the force coefficient for these three gases. One can see that the specific heat ratio has a low influence since monatomic and diatomic gases follow the same trend. The expression for Knudsen force coefficient based on  $Kn$  is

$$C_{Kn} = \frac{1}{AKn^\alpha + BKn^\beta + CKn^\gamma}, \quad (4)$$

where  $A = 38.0535$ ,  $B = 5.6832$ ,  $C = 8.3818$ ,  $\alpha = -0.3835$ ,  $\beta = -2.3362$ , and  $\gamma = 0.8549$ .

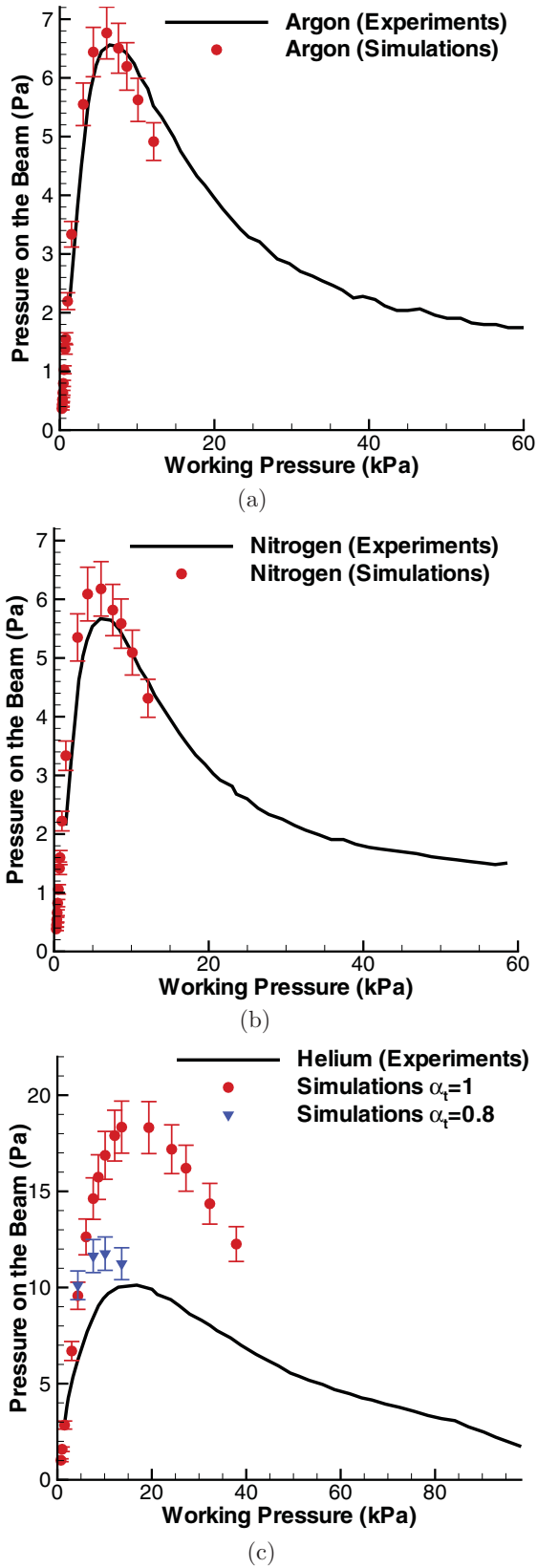


FIG. 4. (Color online) Comparison of Knudsen force simulations with experimental data [5]. (a) Argon, (b) nitrogen, and (c) helium. The error bars were calculated using Richardson extrapolation on three different meshes.

In practical applications, it is desirable to have an expression for Knudsen force for an arbitrary temperature ratio between the beam and the substrate. The influence of the temperature ratio between the beam and the substrate has been investigated by running simulations for  $\frac{T}{\Delta T}$  ranging from 0.75 to 60 [Fig. 5(b)] while keeping the Knudsen number fixed at  $Kn = 2$ . The deviation from  $\frac{T}{\Delta T} = 10$ , which corresponds to the value at which Eq. (4) was derived, is then used to obtain an expression for a correction factor,

$$\alpha_{Kn} = D \left( \frac{T}{\Delta T} \right)^\delta + E \left( \frac{T}{\Delta T} \right)^\epsilon, \quad (5)$$

where  $D = -0.9146, E = 0.6203, \delta = -0.4224$ , and  $\epsilon = -0.2602$ . Thus, the force coefficient for an arbitrary temperature ratio may be obtained by multiplying Eq. (4) by the correction factor given in Eq. (5).

As seen on Fig. 5(a), the experimental results start to deviate from the simulations when the Knudsen number is greater than 1. The microbeam used in the experiments [5] had a series of small holes with a diameter of approximately  $2 \mu\text{m}$ . When the mean free path becomes larger than the hole diameter, the flow conductance through the holes decreases. The effective front-to-side ratio of the beam starts to deviate from the value of 10 assumed in the 2D simulations. Note that the experimental measurements for helium when cast in the nondimensional form show a distinctly different slope at low Knudsen numbers than those for argon and nitrogen. This underlines the effect on Knudsen force of the incomplete accommodation of helium gas interacting with a silicon surface.

The compact model for the nondimensional Knudsen force coefficient can be used for common gases, such as argon, nitrogen, air, and other gases, to quantify the magnitude of Knudsen force for various thermal, pressure, and geometric conditions. This applies even to conditions outside of the ranges for which the experimental data exist now, as long as the interaction between the gas and the beam surface is known to be fully diffuse. This is true for most microscopically rough surfaces interacting with common inert gases. However, for the few light gases such as helium or for atomically smooth surfaces, the incomplete accommodation has to be accounted for.

#### IV. CONCLUSIONS

The numerical solutions of Boltzmann-ESBGK equation have been compared with experimental measurements for the Knudsen force on heated microcantilevers for different gas compositions and pressures. It has been shown that the force is not a consequence of a difference in energy accommodation coefficient on the top and bottom surfaces of the cantilever, but a result of a more general nonequilibrium thermal transport even at a constant and full accommodation. The study showed that the numerical modeling with full accommodation for argon and nitrogen agrees well with measurements, whereas the measurements for helium are lower than the simulation predictions due to incomplete momentum accommodation. A closed-form model for Knudsen force dependence on pressure, geometry, and temperature difference has been obtained in a nondimensional form for application in design and analysis of microsystems.

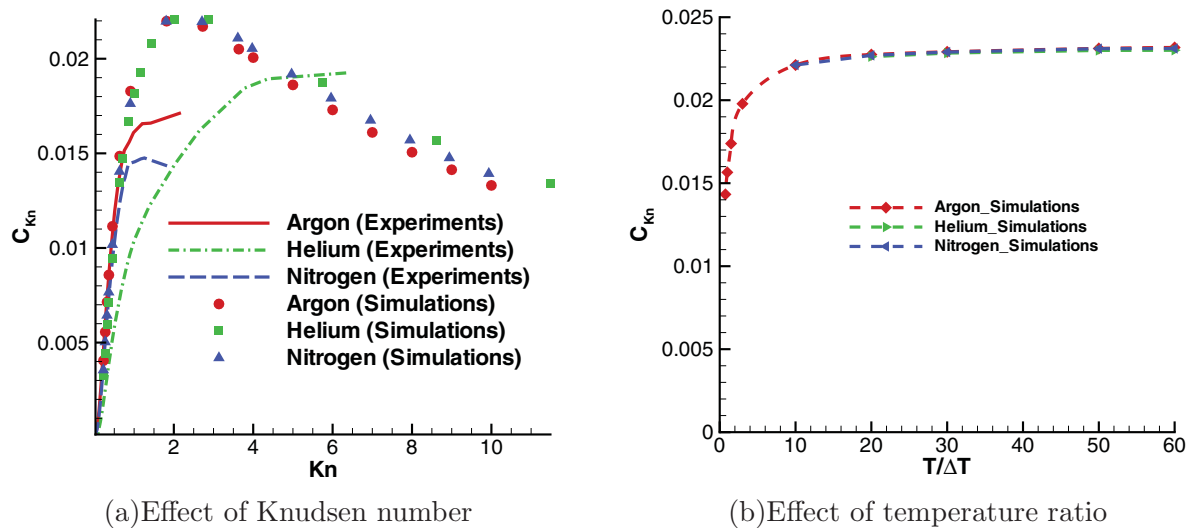


FIG. 5. (Color online) Comparison of the force coefficient based on simulations with experimental results. The experimental values deviate when  $Kn > 1$ , that is, mean free path is larger than set of  $2\text{-}\mu\text{m}$  holes. Though the dimensional force in newtons is different for the three gases (argon, nitrogen, and helium), the coefficient of Knudsen force collapses neatly into a single line with the compact form as in Eq. (3).

**ACKNOWLEDGMENTS**

This work was supported in part by National Science Foundation CBET Grant No. 1055453. The development of the Boltzmann-ESBGK solver was supported in part

by Purdue’s Computing Research Institute and the NNSA Center for Prediction of Reliability, Integrity and Survivability of Microsystems (PRISM) under Contract No. DE-FC52-08NA28617.

[1] C. Draper, *J. Chem. Educ.* **53**, 356 (1976).  
 [2] Y. Wu, *Ann. Phys. (Weinheim, Ger.)* **474**, 144 (1967).  
 [3] F. C. Tompkins and D. E. Wheeler, *Trans. Faraday Soc.* **29**, 1248 (1933).  
 [4] N. Selden, C. Ngalande, S. Gimelshein, E. P. Muntz, A. Alexeenko, and A. Ketsdever, *Phys. Rev. E* **79**, 041201 (2009).  
 [5] A. Passian, R. J. Warmack, T. L. Ferrell, and T. Thundat, *Phys. Rev. Lett.* **90**, 124503 (2003).  
 [6] A. Passian, R. Warmack, A. Wig, R. Farahi, F. Meriaudeau, T. Ferrell, and T. Thundat, *Ultramicroscopy* **97**, 401 (2003).  
 [7] A. A. Alexeenko, E. P. Muntz, M. A. Gallis, and J. R. Torczynski, in *Proceedings of 36th AIAA Fluid Dynamics Conference, San Francisco, CA, AIAA Paper 2006-3715* (AIAA, Reston, VA, 2006), pp. 1907–1915.  
 [8] T. Zhu and W. Ye, *Phys. Rev. E* **82**, 036308 (2010).  
 [9] Y. Sone, *Molecular Gas Dynamics: Theory, Techniques, and Applications* (Birkhauser, Boston, 2007).  
 [10] A. Passian, A. Wig, F. Meriaudeau, T. Ferrell, and T. Thundat, *J. Appl. Phys.* **92**, 6326 (2002).  
 [11] P. Andries, P. Le Tallec, J. Perlat, and B. Perthame, *Eur. J. Mech. B Fluids* **19**, 813 (2000).  
 [12] A. Alexeenko, S. Gimelshein, E. Muntz, and A. Ketsdever, *Int. J. Therm. Sci.* **45**, 1045 (2006).  
 [13] A. A. Alexeenko, in *Proceedings of the 25th International Symposium on Rarefied Gas Dynamics* (Siberian Branch, Russian Academy of Sciences, Novosibirsk, 2007), pp. 184–196.  
 [14] K. Aoki, Y. Sone, and N. Masukawa, in *Proceedings of the 19th International Symposium on Rarefied Gas Dynamics* (Oxford University Press, Oxford, 1995), Vol. 1, pp. 35–41.  
 [15] N. Selden, N. Gimelshein, S. Gimelshein, and A. Ketsdever, *Phys. Fluids* **21**, 073101 (2009).  
 [16] W. Curtis, J. Logan, and W. Parker, *Linear Algebra Its Appl.* **47**, 117 (1982).